Solution Properties of Xanthan. 2. Dynamic and Static Light Scattering from Semidilute Solution

T. Coviello,† W. Burchard,* M. Dentini,† and V. Crescenzi†

Institute of Macromolecular Chemistry, University of Freiburg, 7800 Freiburg, FRG.
Received July 17, 1986

ABSTRACT: Semidilute solutions of "native" xanthan (product of Kelco), pyruvate-free xanthan, and acetate-free xanthan have been studied by static and dynamic light scattering up to values of $X = 20$, where $X = A_2M_wc/[^9/_{16} - (\ln M_w/M_n)/8] \sim c/c^*$. The osmotic compressibility $(M/R_{gas}T)(\partial\pi/\partial c)$ exhibits a significantly weaker increase for these stiff chains than that predicted by the renormalization theory of Ohta and Oono and that found for flexible chains. The concentration dependence of the cooperative diffusion coefficient is again weaker than for polystyrene chains and other flexible polymers, and it is considerably lower than predicted by a recent theory of Oono et al. The time correlation functions can for each concentration be reduced to angular-independent shape functions $\zeta(\Gamma t,c)$ if scaling with respect to $\Gamma = -\partial \ln g_1(t)/\partial t$ at $t = 0$ is applied. These shape functions develop an increasingly large tail at long delay times. This tail is considerably more pronounced than that predicted by Doi and Edwards for rigid rods in the semidilute regime. This longer tail is attributed to an enhanced entanglement as the result of the remaining partial flexibility of the xanthan chains.

Introduction

The study of semidilute solutions of polymers has enjoyed increasing interest in recent years. This interest and the resulting activity in this field have different roots. One is the discovery that the structure of a semidilute solution is a pecularity of polymers that does not occur with low molecular weight compounds.[1,2] Another root originates from the development of dynamic light scattering (DLS), or photon correlation spectroscopy, as a new technique for polymer characterization.[3] In DLS, no external force is employed to the system and all dynamic quantities are obtained from the segment density fluctuations around the equilibrium mean.

We have recently studied various types of polymers by dynamic light scattering in a concentration range from the typical dilute regime up to about 10–20 times the coil-overlap concentration c^*. These studies include typical flexible chains[4,5] with Kuhn segment lengths around l_k = 2.4 nm, a 12-arm polystyrene star[6] and a semiflexible cellulose derivative with a Kuhn length of 22 nm.[7] We now report the behavior of very rigid chains in the semidilute region. In the previous paper[8] the Kuhn lengths of "native" xanthan (NX), (product of Kelco), of pyruvate-free xanthan (PFX), and acetate-free xanthan (AFX) were determined (NX, $l_k = 255 \pm 15$ nm; PFX, $l_k = 310 \pm 40$ nm; AFX, $l_k = 198 \pm 13$ nm). The studied chains were found to be composed of 6.3 ± 0.6 (NX), 3.5 ± 0.4 (PFX), and 5.5 ± 0.4 (AFX) Kuhn segments, respectively. (Xanthan is a polysaccharide with a cellulose backbone; its structure was given in ref 8. The present products have polydispersities of $M_w/M_n = 2$.) Chains of such a low number of Kuhn segments no longer can achieve Gaussian statistics. The purpose of this paper is now the study of the influence of chain stiffness on the semidilute behavior.

Predicted Properties

We are aware of the fact that presently no theory is available that would predict the properties of semiflexible or wormlike chains in the semidilute concentration regime of entanglement. It nevertheless will be useful to review in brief some properties that have been predicted by des Cloiseaux[1] and de Gennes[2] for *flexible chains in a good solvent*. These relationships are given in de Gennes' well-known book.[2] When comparing these equations with our experimental data from the stiff xanthans, we do not expect agreement; the purpose of such a comparison is to show in which direction deviations occur from this reference system of flexible chains. We take here the view of a pure experimentalist and hope that the results may stimulate theoreticians to derive relationships for a consistent interpretation.

Semidilute solutions are of rather low concentrations but nevertheless show a significant difference in behavior compared to typical dilute solutions. The change in properties occur around the *coil-overlap concentration* c^*, which may be defined by

$$c^* = (3/4\pi)(M/N_AR_h^3) \tag{1}$$

where R_h is the hydrodynamic radius, which can be obtained from diffusion measurements (see eq 8). This definition of c^* is only one of many which differ, however, only by constant factors.

A second important quantity is the *correlation length* ξ. The basis of this length results from the assumption that at a concentration $c \gg c^*$ a homogeneous transient network of entangled chains is obtained. The correlation length may then be interpreted as the mean distance between two points of entanglements. Clearly, the correlation length must decrease with increasing concentration and is given by

$$\xi = R(c/c^*)^{-3/4} \tag{2a}$$

where R is the mean end-to-end distance of a single chain in a good solvent.

For the *osmotic pressure*, des Cloiseaux derived[1,2]

$$\pi/R_{gas}T \sim (c/M)(c/c^*)^{1.25} \tag{3}$$

Consequently for the *scattered light* at zero angle, one has

$$Kc/R_{\theta=0} = (1/R_{gas}T)(\partial\pi/\partial c) \sim (1/M)(c/c^*)^{1.25} \tag{4}$$

where K is an optical contrast factor, R_θ the light scattering intensity at the scattering angle θ (Rayleigh ratio), and R_{gas} the gas constant.

Angular Dependence of Scattered Light. On the basis of special assumptions Edwards[9,2] derived for semidilute solutions

$$R_\theta/Kc = g/(1 + \xi_T^2q^2) \tag{5}$$

with

$$q = (4\pi/\lambda)\sin\theta/2$$

$$g = R_{gas}T/(\partial\pi/\partial c) = c\xi_T^3 \sim M(c/c^*)^{-1.25} \tag{6}$$

†Dipartimento di Chimica, Università di Roma "La Sapienza", Italy.

0024-9297/87/2220-1102$01.50/0

Table I
Native Xanthan[a]

10^3c, g/mL	X	M_w/M_{app}	$\langle S^2\rangle_{app}/\langle S^2\rangle_0$	D_c/D_0	$\langle S^2\rangle_c/\langle S^2\rangle_0$	f_0/f_c	ξ_T^*/ξ_h^*
0	0.0	1	1	1	1	1	0.577
0.4	1.22	2.15	0.498	1.30	1.07	0.605	0.529
0.6	1.83	2.73	0.405	1.54	1.11	0.564	0.566
0.8	2.44	3.41	0.340	1.65	1.33	0.472	0.542
1.0	3.05	3.91	0.303	1.93	1.033	0.493	0.613
2.01	6.13	7.64	0.145	2.45	1.11	0.321	0.539
3.0	9.16	10.76	0.109	3.30	1.17	0.307	0.629
6.0	19.3	24.30	0.036	5.10	0.875	0.210	0.559

[a] $X = 1503c$; $M_w = 2.94 \times 10^6$; $D_0 = 1.55 \times 10^{-8}$ cm^2/s; $\langle S^2\rangle_0^{1/2} = 290$ nm; $A_2 = 4.94 \times 10^{-4}$ cm^3/g; $N_k = 6.3$.

Table II
Pyruvate-Free Xanthan[a]

10^3c, g/mL	X	M_w/M_{app}	$\langle S^2\rangle_{app}/\langle S^2\rangle_0$	D_c/D_0	$\langle S^2\rangle_c/\langle S^2\rangle_0$	f_0/f_c	ξ_T^*/ξ_h^*
0	0.0	1	1	1	1	1	0.577
0.4	0.60	1.59	0.552	1.05	0.867	0.669	0.450
0.6	0.90	1.86	0.398	1.20	0.740	0.645	0.437
0.8	1.20	2.14	0.357	1.25	0.764	0.584	0.432
1.04	1.56	2.40	0.273	1.30	0.656	0.542	0.392
2.08	3.13	3.78	0.156	1.51	0.590	0.400	0.344
2.50	3.75	4.46	0.159		0.709		
3.00	4.51	4.80	0.123	1.73	0.590	0.361	0.350
4.80	6.13	7.95	0.080	2.23	0.636	0.281	0.364
5.99	9.00	9.22	0.061	2.58	0.562	0.280	0.368
8.65	13.00	14.47	0.048	3.28	0.694	0.228	0.415

[a] $X = 1503c$; $M_w = 1.37 \times 10^6$; $D_0 = 2.6 \times 10^{-8}$ cm^2/s; $\langle S^2\rangle_0^{1/2} = 240$ nm; $A_2 = 5.22 \times 10^{-4}$; $N_K = 3.5$.

Table III
Acetate-Free Xanthan[a]

10^3c, g/mL	X	M_w/M_{app}	$\langle S^2\rangle_{app}/\langle S^2\rangle_0$	D_c/D_0	$\langle S^2\rangle_c/\langle S^2\rangle_0$	f_0/f_c	ξ_T^*/ξ_h^*
0	0.0	1	1	1	1	1	0.577
0.4	0.893	1.88	0.53	1.09	0.996	0.580	0.458
0.6	1.34	2.30	0.43	1.13	0.989	0.491	0.428
0.8	1.79	2.71	0.34	1.19	0.921	0.439	0.401
1.0	2.23	3.12	0.33	1.23	1.03	0.394	0.408
1.96	4.37	5.49	0.17	1.63	0.933	0.297	0.388

[a] $X = 2232c$; $M_w = 1.77 \times 10^6$; $D_0 = 2.60 \times 10^{-8}$ cm^2/s; $\langle S^2\rangle_0^{1/2} = 210$ nm; $A_2 = 6.00 \times 10^{-4}$ cm^3/g; $N_K = 5.5$.

In this picture g appears as the polymeric mass embodied in a volume that is spanned by the correlation length ξ_T. In contrast to the topologically defined correlation length in eq 2, ξ_T is based on thermodynamic arguments and has the meaning of a shielding length for thermodynamic interactions.

The *dynamic* behavior is governed by the cooperative diffusion which is given by[2]

$$D_c = kT/(6\pi\eta_0\xi_h) \tag{7}$$

This equation defines a hydrodynamically effective correlation length. Since at infinite dilution the translational diffusion coefficient D_0 is related to the hydrodynamic radius of the molecule R_h via the Stokes–Einstein relationship

$$D_0 = kT/(6\pi\eta_0 R_h) \tag{8}$$

we can write

$$D_c/D_0 = R_h/\xi_h = (c/c^*)^{3/4} \tag{9}$$

where instead of eq 2a we have

$$\xi_h = R_h(c/c^*)^{-3/4} \tag{2b}$$

Most of these equations were derived from scaling arguments, which requires $c/c^* \gg 1$. Besides the ambiguity in the exact value of c^*, scaling theory has the disadvantage of predicting only *limiting exponents*. In experiments, however, the whole concentration region from dilute to semidilute behavior is covered, and experimentalists need know more on the amplitude factors and how the asymptotic scaling laws are approached as the concentration passes through the transition zone.

Recently, several analytic expressions have been derived from renormalization group theory for the osmotic pressure and the corresponding derivative that governs the zero-angle scattering intensity. Here we only quote the equation by Ohta and Oono[10,11]

$$(M_w/R_{gas}T)(\partial\pi/\partial c) = 1 + 1/8[9X - 2 + 2\ln(1 + X)/X]\ \exp 1/4[1/X + (1 - 1/X^2)\ln(1 + X)] \tag{10}$$

where M_w is the weight-average molecular weight at infinite dilution. The dimensionless parameter X is uniquely related to the second virial coefficient A_2. Expansion of the above equation near $c = 0$ and comparison with the common virial expansion of the osmotic pressure give

$$X = A_2M_wc/[9/16 - \ln(M_w/M_n)/8] \sim (c/c^*) \tag{11}$$

Thus, the use of X requires the determination of A_2 and M_w. In the following we will use this relationship instead of eq 1, and to avoid confusion, we wish to emphasize that eq 1–11 were derived for *flexible chains*.

Results

Figures 1–3 give the results for NX, PFX, and AFX in a 0.1 M NaCl aqueous solution. The first two figures show the static behavior and the third shows the dynamic behavior. The static and dynamic light scattering measurements were carried out simultaneously with the same light scattering instrument. Reduced quantities were used;

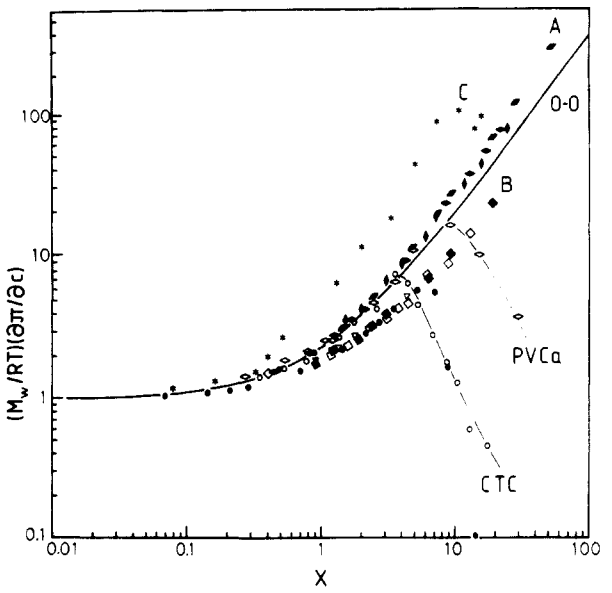

Figure 1. Reduced osmotic compressibility as a function of $X = A_2M_wc/[9/16 - \ln(M_w/M_n)/8]$ for various polymers: (A) linear polystyrenes of different molecular weights in toluene ($N_k > 45$); (B) xanthan chains in 0.1 M NaCl water (◆) NX, (◇) PFX, (▽) AFX; (C) 12-arm polystyrene star molecule in toluene.[6,12] 0–0 indicates the theory by Ohta and Oono.[10] PVCa, poly(vinylcaprolactam) in water at 20 °C; CTC, cellulose tricarbanilate in dioxane at 20 °C; (●) $M_w = 130\,000$ ($N_k = 6.3$); (○) $M_w = 10^6$ ($N_k = 45$).

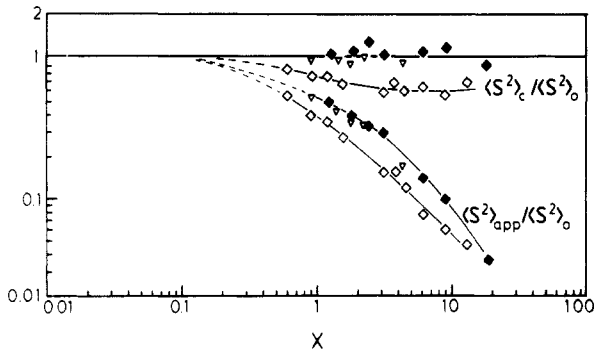

Figure 2. Apparent mean-square radius of gyration $\langle S^2\rangle_{app}$, and $\langle S^2\rangle_c$ (eq 14), normalized by the zero concentration mean-square radius of gyration $\langle S^2\rangle_0$, as a function of X. Symbols as in Figure 1.

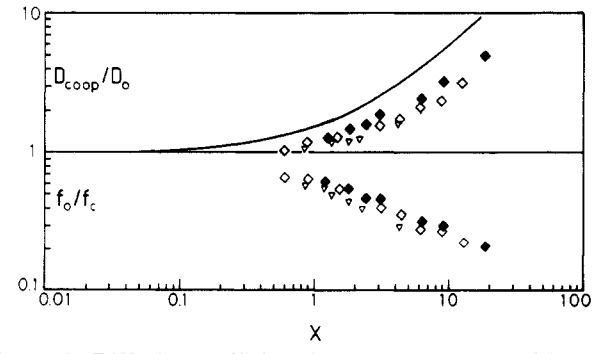

Figure 3. Diffusion coefficient (at zero scattering angle), $D_{coop} = D_c$, upper section, and friction coefficient f_c, lower section, as a function of X for the same xanthans as shown in Figure 1.

i.e., the measured values $(Kc/R_{\theta=0})_c$, $\langle S^2\rangle_c$, and D_c were normalized with respect to the corresponding quantities at infinite dilution and these were plotted against X.

The main results are summarized as follows:

1. Up to the overlap concentration the static and dynamic properties show the typical dilute solution behavior.

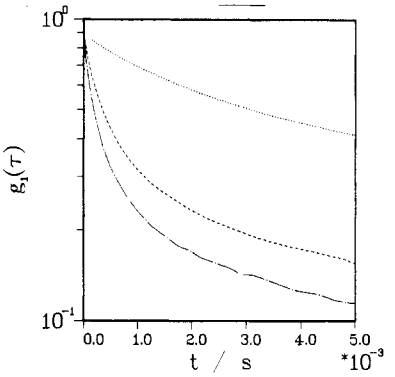

Figure 4. Time correlation functions of PFX solutions at $c = 4 \times 10^{-3}$ g/mL for 30°, 90°, and 130° angles.

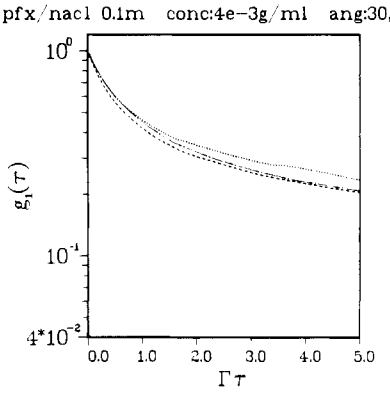

Figure 5. The same correlation functions as shown in Figure 3 but now plotted against $\Gamma\tau$, where Γ is the first cumulant (initial slopes in Figure 4) and τ the delay time (in the text t).

The scattering intensity at zero angle follows the relationship

$$(Kc/R_{\theta=0})_c = (R_{gas}T)^{-1}(\partial\pi/\partial c) = (1/M_w)(1 + 2A_2M_wc + ...) \quad (12)$$

with a vanishing third virial coefficient. Terms of higher power in c become effective at $X > 1$.

2. The normalized zero scattering intensity $(M/R_{gas}T)(\partial\pi/\partial c)$ forms for all xanthans a common line when plotted against the parameter X. The curve shows, however, a weaker increase than predicted by Ohta and Oono[10] for *flexible* chains and a weaker dependence than for chains with more than 45 Kuhn segments, where Gaussian statistics can be assumed to hold.

3. The apparent radius of gyration $\langle S^2\rangle_{app}$ (defined in eq 13) shows a strong concentration dependence, as can be seen from Figure 2. The data for PFX deviate slightly from the curve of NX and AFX, which are doubly stranded chains.[8]

4. The data of D_c/D_0 as function of X do not coincide to the same accuracy and show no significant deviation from the curve obtained for flexible chains.[11,12]

5. The time correlation functions (TCF) have strong angular dependences (Figure 4), but these can be reduced to a common line (Figure 5) if the data are plotted against Γt, where Γ is the first cumulant (initial slope of the logarithmic time correlation function). This master curve will be called in the following a "shape function" $\mathcal{S}(\Gamma t,c)$.

The concentration dependence is best recognized from Figure 6, where the TCFs for five concentrations of PFX are plotted, in logarithmic scale, against Γt. The logarithmic shape function is strongly nonlinear and this nonlinearity becomes more pronounced with increased concentration.

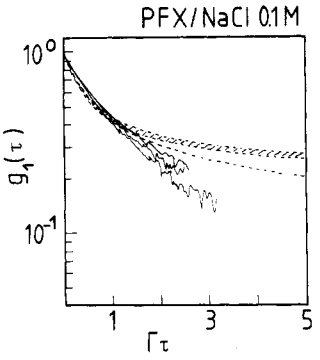

Figure 6. Shape functions of PFX at the five concentrations of 0.4×10^{-3}, 1.04×10^{-3}, 2.08×10^{-3}, 4.8×10^{-3}, and 5.99×10^{-3} g/mL (from below).

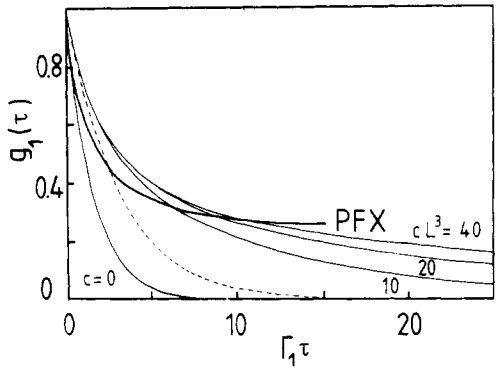

Figure 7. Comparison of the measured TCT for PFX, at 5.99 $\times 10^{-3}$ g/mL, with curves calculated by Doi and Edwards[22] for rods in semidilute solutions. The numbers indicate values of cL^3, where c is the number concentration and L is the contour length. For PFX we find $cL^3 = 79$ if the Kuhn length of 310 nm is taken for L.

Discussion

Osmotic Pressure Gradient. The properties of the semidilute xanthans solutions show behavior that in some respect differs from that observed for all other polymer structures studied in good solvents. Scaling theory predicts for the concentration dependence of the normalized zero-angle scattering intensity a limiting exponent of 1.25 for *flexible* chains. The renormalization group theory by Ohta and Oono[10] reaches this asymptote for $X \simeq 20$. Experiments with high molecular weight polystyrenes show at this point a still-increasing function that at $X = 50$ may be described with an exponent of 1.46 ± 0.02.[12] Curve A of Figure 1 agrees for $X > 0.4$ exceedingly well with that obtained by Wilzius et al.[11] In all these cases the number of Kuhn segments per chain is larger than $N_k = 45$; these polymers represent typical flexible chains.

The corresponding curve B of the three xanthans and one cellulose tricarbanilate chain (CTC) of M_w 131 000[7] shows a remarkably weaker increase of $(M/R_{gas}T)(\partial\pi/\partial c)$ with increasing X; at $X = 20$ it is 3 times smaller than for the flexible chains. The NX, AFX, and CTC chains have approximately the same number of Kuhn segments, i.e., $N_k = 6.3$, 5.5, and 5.9, respectively, while PFX has only 3.5 Kuhn segments per chain. Such polymers no longer follow flexible chain statistics.[8] Curve B gives evidence for a different renormalization behavior if chain stiffness comes into play. Furthermore at $X = 20$ asymptotic scaling behavior is apparently not yet observed. The curvature still increases, and the highest exponent that can be estimated at that point is 1.12 ± 0.02.

Although no theory on semidilute stiff chains is presently available, one may state that the loose coil of a semiflexible chain with its lower average segment density causes less osmotic resistance against coil interpenetration than for the more dense flexible chains. This interpretation is supported by the observation of a much more pronounced increase of the osmotic pressure with increasing X for 12-arm star-branched molecules.[6,12]

Figure 1 shows two further curves with a striking turnover to smaller values. These curves were obtained with CTC in dioxane[7] and poly(vinylcaprolactam) (PVCa)[13] in water. Similar behavior was observed also for some PS molecules in various solvents.[14,15] This turnover has been interpreted by a clustering or association of chains,[6,7] and the phenomenon has been brought into correlation with the capability of these polymers to form real gels at low temperatures. The occurrence of associates may be considered as a system of molecules in a pregel state. In a previous paper we expressed an expectation that such cluster formation might be a general feature of entangled chains in semidilute solutions. However, for the xanthan molecules such cluster formation is not observed in the concentration region of our measurements; also for high molecular weight PS there is no indication for association. Possibly a cluster formation may occur if the *overall* concentration exceeds a certain value which is not yet reached for the present xanthans and the measured high PS molecules.

Radius of Gyration. From the initial slope of the angular dependent curve at a concentration c in the Zimm plot an apparent mean-square radius of gyration $\langle S^2\rangle_{app}$ can be derived with the relationship

$$Kc/R_\theta = (1 + 1/3\langle S^2\rangle_{app}q^2 - ...)/M_{app} \qquad (13)$$

where $1/M_{app} = (R_{gas}T)^{-1}(\partial\pi/\partial c)$ is the intercept of this curve at $q^2 = 0$. The concentration dependence of $\langle S^2\rangle_{app}$ can be discussed on two different lines.

1. The Zimm plots of the scattered light intensities show parallel lines up to the highest concentrations that have been measured. Evidently the Debye equation of light scattering can still be applied to these high concentrations. Under these circumstances we can derive

$$\langle S^2\rangle_{app}/M_{app} = \langle S^2\rangle_c/M_w \qquad (14)$$

or

$$\langle S^2\rangle_c/\langle S^2\rangle_0 = \langle S^2\rangle_{app}/\langle S^2\rangle_0(M_w/R_{gas}T)(\partial\pi/\partial c) \qquad (15)$$

where $\langle S^2\rangle_c$ may be taken as a definition of the mean-square radius of gyration of the chain at the concentration c and $\langle S^2\rangle_0$ is the corresponding radius at $c = 0$. $\langle S^2\rangle_{app}$ is defined by eq 13. The data of $\langle S^2\rangle_c$ which were calculated according to eq 14 are plotted in Figure 2. Only for the PFX is a weak decrease with increasing X observed.

2. In the derivation of Edwards,[9] one has for flexible chains

$$\langle S^2\rangle_{app} = 3\xi_T^2 \qquad (16a)$$

or

$$\xi_T/R_g = (\langle S^2\rangle_{app}/3\langle S^2\rangle_0)^{1/2} \qquad (16b)$$

where $R_g = \langle S^2\rangle_0^{1/2}$ is the radius of gyration at $c = 0$. This result may be compared with the corresponding dynamic correlation length ξ_h.

Diffusion Coefficient. The concentration dependence of the translational diffusion coefficient can be discussed on the same basis as the geometric radius of gyration.

1. Following irreversible thermodynamics one has (neglecting the buoyancy term)[16]

$$D_c = (M_w/N_Af_c)(\partial\pi/\partial c) \qquad (17)$$

or

$$D_c/D_0 = (f_0/f_c)[(\partial\pi/\partial c)(M_w/R_{gas}T)] \qquad (18)$$

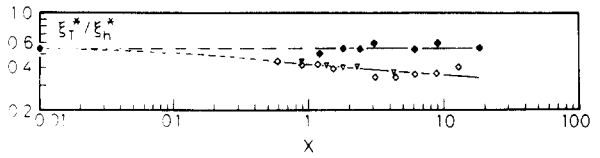

Figure 8. Ratio of the thermodynamic shielding length ξ_T^* to the hydrodynamic correlation length ξ_h^* for the three xanthans.

The term in the square brackets is $M_w Kc/R_{\theta=0}$. Thus by combination of the diffusion and the static light scattering measurements at zero angle the change of the friction coefficient f_c with increasing concentration can be obtained.[17,18] The upper part of Figure 3 represents the data of the diffusion measurements and the lower part exhibits the concentration dependence of the frictional coefficient. The friction increases with X as could be anticipated from physical arguments.

2. On the basis of the de Gennes theory the diffusion coefficient of flexible chains in the semidilute regime is given by eq 9 and 2b; exponential behavior is expected to hold if $c \gg c^*$; i.e., $X \gg 1$. Combination of eq 9 with eq 5 gives

$$\xi_T^*/\xi_h^* = (D_c/D_0)(\langle S^2\rangle_{app}/3\langle S^2\rangle_c)^{1/2} \quad (19)$$

with

$$\xi_T^* = \xi_T/R_g$$

$$\xi_h^* = \xi_h/R_h$$

where $R_g = \langle S^2\rangle_0^{1/2}$ and R_h are the geometric and hydrodynamic radii at zero concentration. It is generally assumed that the thermodynamic shielding length ξ_T and the hydrodynamic correlation length ξ_h may not be identical in value but nevertheless will show the same concentration dependence. This assumption is verified with the native xanthan. In the two other cases ξ_h shows a weaker decrease with c than ξ_T and demonstrates the need for distinguishing both quantities, even in good solvent systems. See Figure 8.

The highest exponent ν in the relationship

$$D_c/D_0 \sim X^\nu \quad (20)$$

measured at $X = 20$ is for the three xanthans $\nu = 0.60 \pm 0.02$, which is lower than the value of 0.75 predicted for flexible chains at large X.

Recently Oono et al.[19] derived for flexible chains a closed formula for D_c/D_0 on the basis of renormalization group theory. This equation was expanded and truncated after the linear term in c with the result

$$D_c/D_0 = Kc + \ldots \quad (21)$$

$$Kc = [\exp(Y) - 3Y/(1 - (1 + \zeta)^{-3/4})]X \quad (22)$$

with[20]

$$Y = \zeta/(8(1 + \zeta)) \quad (23)$$

$$\zeta = 32z/3 \quad (24)$$

and where z is the well-known interaction parameter.[21,16]

Wiltzius et al. observed a clear chain length and solvent dependence of D_c/D_0 and contributed this to different "crossover" behavior to marginal excluded volume effect and partial draining. In the Oono et al.[19] theory this crossover is expressed by the z parameter in eq 23, ($z \to \infty$ corresponds to maximum excluded volume effect and $z = 0$ to Θ conditions). However, unrealistically low values of $z = 1$ and 0.1 had to be assumed to describe satisfactorily the experimental curve. In Figure 3 we plotted the curve for $z = \infty$, which gives

$$D_c/D_0 = 1 + [\exp(1/8)\zeta - 3/8]X = 1 + 0.5075X \quad (25)$$

This relationship gives a much too strong increase of the diffusion coefficient with concentration compared to the experimental curve obtained for the xanthans. Agreement of the experimental data for xanthan with eq 25 was not expected since the xanthan chains are typical stiff chains whereas eq 25 was derived for flexible chains in the limit of $z = \infty$ (good solvent). Although a theory for stiff chains in semidilute solution is missing it remains of interest to compare the experimental results with those obtained with flexible chains. In no case the predicted strong increase of D_c/D_0 was observed, and all measurements made from polymers, whatever the architecture, show no significant differences in their concentration dependences.[11,12]

We may briefly summarize the results and add some speculative arguments.

1. The normalized osmotic compressibility $(M/R_{gas}T)(\partial\pi/\partial c)$ can be measured by means of light scattering. The experimental data for *flexible* chains form one common curve when plotted against the parameter $X = A_2 M_w c \sim c/c^*$, where c^* is the overlap concentration. The shape of this curve is independent (i) of the chemical composition of the chains, (ii) of the solvent quality, as long as $A_2 > 0$, and (iii) of the molecular weight, as along as the chains consist of more than 45 statistical Kuhn segments.

2. The curve of the osmotic compressibility runs below this line if the chains are considerably shorter than 45 Kuhn segments. Again, chains of different chemical structure form a common curve if they consist of approximately the same number of Kuhn segments. Polydispersity has only little influence on the shape of the curves.[11]

3. The observed deviations from the osmotic compressibility of flexible chains could be caused by a prefactor in the parameter X which may depend on the number of Kuhn segments and probably also on the length of the Kuhn segment, but the results may intuitively also be interpreted by assuming that stiff chains can more easily be forced to interpenetrate than flexible chains.

4. The cooperative diffusion coefficients D_c of the stiff chains show similar behavior to those of flexible chains. No scaling behavior is observed for the flexible as well as for the stiff chains if X is used as the only scaling parameter. The breakdown of scaling may result from a marginal excluded volume effect but also from a partial draining effect.

5. The thermodynamically defined equilibrium shielding length ξ_T is found not to be proportional to the hydrodynamic correlation length ξ_h. This observation gives evidence for a hydrodynamic interaction that varies in a different manner with concentration than the equilibrium shielding length.

6. The time correlation function of the dynamic light scattering shows for the measured xanthans a strong angular dependence. This angular dependence can be transformed into an angular-independent shape function if the correlation time is scaled with respect to the first cumulant, $\Gamma = -\partial \ln (g_1(t),c)/\partial t$ at $t = 0$. This scaling behavior indicates that within the experimentally covered angular range the correlation function is determined by a spectrum of *internal* relaxation times.

Acknowledgment. W.B. thanks Professor K. F. Freed, University of Chicago, for several helpful comments and for drawing attention to two very recent papers by Douglas et al.[25] and Cherayil et al.[26] These two papers have not

been considered in the present contribution but may be helpful for a more quantitative interpretation of the experimental findings. The work was kindly supported by Maizena Industrial Products, Hamburg, and the Deutsche Forschungsgemeinschaft within the scheme SFB 60.

Registry No. NX, 11138-66-2.

References and Notes

(1) des Cloiseaux, J. *J. Phys. (Les Ulis, Fr.)* **1982**, *36*, 281.
(2) de Gennes, P.-G. *Scaling Concepts in Polymer Physics*; Cornell University Press: Ithaca, NY, 1979.
(3) Burchard, W. *Chimia* **1985**, *39*, 10.
(4) Burchard, W.; Eisele, M. *Pure Appl. Chem.* **1984**, *56*, 1379.
(5) Eisele, M.; Burchard, W. *Macromolecules* **1984**, *17*, 1636.
(6) Huber, K.; Bantle, S.; Burchard, W. *Macromolecules* **1986**, *19*, 1404.
(7) Wenzel, M.; Burchard, W.; Schätzel, K. *Polymer* **1986**, *27*, 195.
(8) Coviello, T.; Kajiwara, K.; Burchard, W.; Dentini, M.; Crescenzi, V. *Macromolecules* **1986**, *19*, 2826.
(9) Edwards, S. F. *Proc. Phys. Soc., London* **1985**, *83*, 5293.
(10) Ohta, T.; Oono, Y. *Phys. Lett.* **1982**, *89A*, 460.
(11) Wiltzius, P.; Haller, H. R.; Cannell, D. S.; Schaefer, D. W. *Phys. Rev. Lett.* **1983**, *51*, 1183.
(12) Burchard, W., to be published.
(13) Eisele, M.; Burchard, W., to be published.
(14) Dautzenberg, H. (a) *Faserforsch. Textilchem.* **1970**, *21*, 341; (b) *J. Polym. Sci.* **1977**, *61*, 83; (c) *Faserforsch. Textilchem.* **1975**, *26*, 551.
(15) Koberstein, J. T.; Picot, C.; Benoit, H. *Polymer* **1985**, *26*, 673.
(16) Yamakawa, H. *Modern Theory of Polymer Solutions*; Harper & Row: New York, 1971.
(17) de Gennes prefers in his book the use of the sedimentation coefficient, which is related to the friction coefficient by the relationship $s = M/f_c$.
(18) de Gennes, P.-G. *Scaling Concepts in Polymer Physics*; Cornell University Press: Ithaca, NY, 1980.
(19) Oono, Y.; Baldwin, P. R.; Ohta, T. *Phys. Rev. Lett.* **1984**, *53*, 2149.
(20) Freed, K. F. *J. Chem. Phys.* **1983**, *79*, 6357.
(21) Zimm, B. H.; Stockmayer, W. H.; Fixman, M. *J. Chem. Phys.* **1953**, *21*, 1716.
(22) Doi, M.; Edwards, S. F. *J. Chem. Soc., Faraday* Trans. *2* **1978**, *74*, 560.
(23) Albrecht, A. C. *J. Chem. Phys.* **1957**, *27*, 1014.
(24) Flory, P. J.; Bueche, A. M. *J. Polym. Sci.* **1958**, *27*, 219.
(25) Douglas, J. F.; Wang, S.-Q.; Freed, K. F. *Macromolecules* **1986**, *19*, 2207.
(26) Cherayil, S. J.; Bawendi, M. G.; Miyake, A.; Freed, K. F. *Macromolecules* **1986**, *19*, 2770.

Theory of Dynamic Scattering from Ternary Mixtures of Two Homopolymers and a Solvent

M. Benmouna,† H. Benoit, M. Duval,* and Z. Akcasu‡

Institut Charles Sadron (CRM-EAHP) CNRS-ULP, 67083 Strasbourg Cedex, France.
Received July 15, 1986

ABSTRACT: The random phase approximation technique, which has been used previously for static and some dynamical problems, is extended to the case of a mixture of two polymers in a solvent. The expressions of intermediate scattering functions obtained are valid at any concentration and for any mixture of monodisperse systems. The main result of this work is that there are two relaxation processes, which we have interpreted as cooperative and interdiffusion modes. The variations of amplitudes and decay rates of these modes with the composition are discussed. Two simple cases are considered in detail: (i) two interacting polymers of the same size but different contrast factors, (ii) a model for a bimodal molecular weight distribution obtained with two monodisperse polymers differing in molecular weight but otherwise identical. It is shown that it is possible to find conditions in which the two modes are identified.

I. Introduction

In recent years, there has been a growing interest in the scattering properties of ternary mixtures of two homopolymers and a solvent from both static[1,2] and dynamic[3-5] points of view. We have recently developed a theory of elastic scattering from such systems that is valid not only in the thermodynamic limit of forward scattering (i.e., zero angle) but also at any angle θ or wave vector $q = (4\pi/\lambda) \sin \theta/2$, where λ is the wavelength of the incident radiation. This theory predicts the essential features of the experimental data for mixtures of homopolymers in solution and, in certain cases, a reasonable quantitative agreement is obtained.[6] The present work attempts to generalize this theory for dynamical properties of such systems. First, we present the general formalism, which can be applied to an arbitrary mixture of homopolymers. Since it is difficult to extract the physical implications from general formulas, two particular practical examples are considered.

The first one is for a mixture of two polymers having the same molecular weight and dimensions but differing in their indices of refraction or contrast factors. We assume that we remain in the range of concentration and compatibility for which we have an homogeneous solution. In the second example, we investigate the effect of polydispersity for the case of two polymers with different molecular weights but otherwise identical. Both problems have been examined in the bulk limit[3] and in the dilute regime.[7] Here, we make an attempt to generalize these results at any concentration, within the framework of Ornstein–Zernike[8] theory or random phase approximation (RPA). The spirit of this approximation is to express the total intensity scattered by various species in the system, taking into account their interactions, in terms of the scattered intensity by the individual molecules. To make this clearer, let $S_{ii}(q)$ denote the static intensity scattered by the molecules of species i. $S_{ii}(q)$ is, in general, a sum of the intensity $S_{ii}^0(q)$ scattered by individual molecules and the contribution $Q_{ii}(q)$ due to the interactions between these molecules, i.e.

$$S_{ii}(q) = S_{ii}^0(q) + Q_{ii}(q) \tag{1}$$

Furthermore, interactions between different species i and j contribute to the total intensity through the quantity

$$S_{ij}(q) = Q_{ij}(q) \qquad (i \neq j) \tag{2}$$

† Permanent address: INES Sciences Exactes, Department of Chemistry, Tlemcen, Algérie.
‡ Permanent address: Department of Nuclear Engineering, The University of Michigan, Ann Arbor, MI 48109.

0024-9297/87/2220-1107$01.50/0